Design and Evaluation of a Human-in-the-Loop Connected Cruise Control

Zheng Chen, Byungkyu Brian Park, *Senior Member, IEEE*, and Jia Hu, *Member, IEEE*

***Abstract*—The performance of automated vehicle can be greatly improved by enabling vehicle-to-vehicle communication. An example of such applications is Cooperative Adaptive Cruise Control (CACC) along the highway. Although the adoption rate of vehicular connectivity is predicted to grow rapidly, CACC can only benefit vehicles that are both connected and automated. To take a full advantage of vehicular connectivity, a human-in-the-loop Connected Cruise Control (hCCC) algorithm is developed for human-driven connected vehicle. In hCCC, the human driver remains engaged in the longitudinal control of the vehicle, and hCCC controller applies additional acceleration/deceleration on top of human actions according to the received status of preceding vehicle. By allowing coexistence of the automatic control and driver's actions in a beneficial way, hCCC helps the human driver stabilize the vehicle more efficiently and safely. The proposed hCCC inherits the feedback-feedforward control structure and velocity-dependent spacing policy from the typical CACC systems. String stability analysis shows that hCCC can offer broader string-stable ranges of human parameters than human driving alone or the existing acceleration-based Connected Cruise Control (CCC), indicating a better capability to mitigate traffic disturbance with the uncertain human behaviors. The desirable properties of hCCC were validated in driving simulator experiments, which showed that hCCC could reduce 36.8% acceleration, 31.2% time-gap fluctuation, 81.2% exposure time to unsafe driving situations, and 15.8% fuel consumption from those of human driving alone. In addition, two derivative designs of hCCC are proposed and proven effective, further lowering down the practice threshold of hCCC.**

***Index Terms*—Connected vehicle, connected cruise control human driver, string stability.**

I. Introduction

As ONE of the basic Automated Vehicle (AV) applications, Adaptive Cruise Control (ACC) has been commercialized and equipped in a portion of new cars [1]. Using onboard sensors (e.g., radar or lidar), ACC can automatically regulate the vehicle's longitudinal motion to maintain a safe gap from the preceding vehicle, thus the labor intensity of drivers can be greatly reduced. However, ACC has been heavily criticized for its poor "string stability", which refers to the property to attenuate the traffic disturbance from downstream [2], [3]. As ACC vehicles tend to be string-unstable, the speed/spacing fluctuations from the preceding vehicle would be amplified, causing shockwaves along the upstream. This problem can be resolved by upgrading ACC to Cooperative ACC (CACC) with connectivity. Using both onboard sensors and vehicle-to-vehicle (V2V) communications, CACC vehicles can obtain the preceding vehicle's states or intentions immediately, and form compact platoons in headways as short as 0.6s, with improved string stability, fuel efficiency and roadway throughput [4]–[6]. Nevertheless, a low usability of CACC in the near future can be expected as it only applies to Connected and Automated Vehicles (CAVs) [4], [7].

While a high Market Penetration Rate (MPR) of CAV cannot be immediately achieved, governments and manufacturers worldwide are making efforts to promote vehicular connectivity [8]. It has been predicted [9] that the MPR of Connected Vehicles (CV) in the U.S. would grow to be greater than 34.8% in 2025. More recently, China released a roadmap [10] that 50% newly manufactured vehicles in China will be line-fitted with connectivity by 2025, and almost all vehicles will be equipped by 2030. However, this does not necessarily mean that CAVs would dominate the market. The MPR of ACC in the U.S. is predicted to be far less than 100% in 2025, and even no greater than that of CVs [9]. A common expectation in previous studies [9], [11], [12] is that there would be a large number of human-driven CVs in the traffic. On one hand, many connected vehicles would not be automated due to the relatively high cost of onboard sensors [9]. On the other hand, CAVs might degrade to manual mode sometimes when the CACC system does not satisfy the driver, who thus prefers to be in control of the vehicle. Such "intended disengagement" has been frequently occurring to Level 1∼2 automated driving applications [13].

While these human-driven CVs (including degraded CAVs) can still facilitate the use of CACC on other vehicles by broadcasting "here I am" messages [4], there would be no direct benefit for themselves. Being always leading vehicles of platoons, human-driven CVs have neither a crisper response to preceding vehicle's maneuvers nor a fuel saving as the CAV followers do [14]. To fully take advantage of vehicular connectivity, human-driven CVs should be able to receive assistance via the connectivity, instead of being just "information providers."

Manuscript received 25 September 2021; revised 8 March 2022; accepted 6 April 2022. Date of publication 9 May 2022; date of current version 15 August 2022. This work was supported in part by the National Science Foundation under Grant CMMI-2009342, in part by the Shanghai Municipal Science and Technology Major under Project 2021SHZDZX0100, in part by the Shanghai Oriental Scholar (2018), Tongji Zhongte Chair Professor Foundation under Grant 000000375-2018082, and in part by the Fundamental Research Funds for the Central Universities. The review of this article was coordinated by Prof. Jianjun Lei. *(Corresponding author: Jia Hu.)*

Zheng Chen is with the PCI Technology Group Co., Ltd., Guangzhou 510000, China (e-mail: zc4ac@virginia.edu).

Byungkyu Brian Park is with the Engineering Systems and Environment Department, University of Virginia, Charlottesville, VA 22904 USA (e-mail: bp6v@virginia.edu).

Jia Hu is with the College of Transportation Engineering, Tongji University, Shanghai 201804, China (e-mail: hujia@tongji.edu.cn).

Digital Object Identifier 10.1109/TVT.2022.3172507

Although a few of applications for human-driven CV have been proposed, they are mostly focused on driver advisory systems for very limited situations. A representative application is CV-based eco-driving system [15] that aims for improving fuel economy when the CV approaches a signalized intersection. It utilizes vehicle-to-infrastructure (V2I) communication to obtain signal phase and timing information, and accordingly recommends the optimal speed to drivers. Other CV-based applications include lane changing advisory system [16] which attempts to reduce merging conflicts around on-ramp by encouraging early mainline freeway lane changes, and cooperative collision warning system [17] which alerts the driver when a highly potential collision is projected using V2V communication. Obviously, the benefits of these advisory systems are subject to human driver's compliance level. The received information in these systems is only used to generate suggestions to the drivers, instead of helping them directly.

A possible step forward from advisory systems is to allow the coexistence of automatic control and driver's actions in a beneficial way. This collaboration between machine and human has become technically and economically feasible with the adoption of electronic actuators in modern vehicles. Electronic throttle [18] has been applied to almost every car. The recent generation of Electronic Stability Program/Control (ESP/ESC) [19], which enables programmed brake control, has also been massively adopted in new cars. Furthermore, there are increasing number of hybrid/electric vehicles equipped with drive-by-wire [20], [21] technology. These electronic actuators can sense human's will through pedals, monitor vehicle's status, and apply corresponding actions on throttle/brake. They not only help drivers achieve their intention faster and more precisely, but also provide the vehicle's software with the convenience to modify or override human's initial action when necessary. This means the additional investment in automatic actuators is no longer needed for many vehicles.

A preliminary design of such system is acceleration-based Connected Cruise Control (CCC) [22]. It proposed to aid the connected vehicle (either automated or human-driven) with an extra acceleration, which is proportional to the acceleration of the preceding vehicle or vehicles. CCC [22] assumed that the human's driving behaviors can be represented by a linearized optimal velocity model (OVM) which regulates the inter-vehicle gap and relative speed from the preceding vehicle. Thus, by applying an extra acceleration feedback, the CCC vehicle can gain a "phase lead" when responding to the speed fluctuations from downstream. Theoretical analysis and numerical simulation indicated that the extra acceleration could help stabilize initially string-unstable vehicle platoons. However, this CCC has never been evaluated with real human drivers, while it was designed and analyzed with a strong assumption that human's behavior patterns are known and unaffected by the extra acceleration. Although more sophisticated CCC systems [23]–[25] were developed to handle the uncertainties in communication delay, human's driving behaviors and communication topology, they focused on an automated ego vehicle and were not designed in the human-in-the-loop fashion.

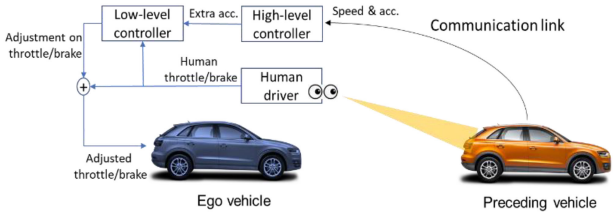

Fig. 1. Framework of hCCC system.

In this study, a human-in-the-loop Connected Cruise Control (hCCC) dedicated for human-driven CVs is proposed. This new driving mode significantly improves the efficiency and safety of human driving by using the vehicular connectivity, even though the vehicle is not automated with a perceptive system (e.g., range sensors). Compared to the existing acceleration-based CCC[22], the proposed hCCC inherits from CACC the feedback-feedforward control structure and zero-spacing-error rule in control design, instead of simply offering a proportion of preceding vehicle' acceleration. Besides, hCCC would bear the following features:

- Utilizing both the speed and acceleration information of preceding vehicle in pursuit of the best performance
- Considering the potential effect of hCCC on the human's behavior
- Less driving load on human
- Less fluctuation in both speed and headway

The effectiveness of hCCC is to be shown by high-fidelity simulations using physics-based vehicle model, real-world vehicle trajectory data, and driving simulator with real human.

The rest of the paper is organized as follows: the Section II explains the human's car-following behavior and the corresponding designs of hCCC algorithm. The theoretical analysis on the string stability of hCCC algorithm is presented in Section III. Section IV investigates the effectiveness of hCCC through human-in-loop experiments, and further discusses some derivative designs of hCCC. The key findings and concluding remarks are provided in Section V.

II. Control Design

The scheme of hCCC system is shown in Fig. 1. The most basic and frequently used communication topology, i.e., predecessor-following (PF) topology [26] is considered in this study. The ego vehicle is assumed to be connected but not automated and with no radar installed. When the ego vehicle is following another CV, the human driver can choose to turn on hCCC and co-pilot the vehicle. On the human side, the driver is still responsible of monitoring the preceding vehicle and giving input to throttle/brake pedals. On the hCCC side, the information of preceding vehicle is retrieved via V2V communication, based on which the extra acceleration (on top of human actions) would be imposed on the ego vehicle to assist the human driver. Due to the nonlinearity of vehicle dynamics, bi-level control design is needed. The high-level controller decides the desired extra acceleration according to the received information of preceding vehicle, and the low-level controller determines how to adjust

the throttle and brake to achieve this extra acceleration. The final inputs to the ego vehicle would be the summation of human's on-pedal throttle/brake and the adjustment made by low-level controller.

The three key components of hCCC design are described respectively in this section, including the method to consider human behavior, and designs of high/low-level controls.

A. Human Driver Consideration

The linearized optimal velocity model (OVM) [24] is adopted to describe car-following behavior of human drivers around a traffic equilibrium:

$$h\left(t\right) = x_2\left(t\right) - x_1\left(t\right) - l$$
$$\ddot{x}_1(t) = \alpha\left(\frac{1}{t_h}h\left(t-\varphi\right) - \dot{x}_1\left(t-\varphi\right)\right) + \beta\dot{h}\left(t-\varphi\right) \quad (1)$$

Where t is time, $\dot{*}$ denotes the variable's derivative in respect to time, $x_1(t)$ and $x_2(t)$ are locations of ego vehicle and preceding vehicle, h is the adjustable gap between the two vehicles, with l being the minimum bumper-to-bumper distance, α and β are human control gains, φ is the human delay (i.e., reaction time), $\frac{1}{t_h}$ is spacing policy slope with t_h being the desired time gap of the human driver. Model (1) indicates that the human driver desires a velocity-dependent spacing, and regulates the spacing error and speed difference from the preceding vehicle simultaneously.

Note that the human parameters in OVM vary from person to person, and even for one single driver, they change stochastically over time. The reference [27] proposed a method trying to address stochastic behavior of driver by measuring the distributions of the human parameters based on the received speed and GPS location of the preceding vehicle, and then representing the stochastic human parameters by constant mean values of α, β, $\frac{1}{t_h}$, and probability density function (PDF) of φ. However, this approximation may be insufficient for control design, because the fluctuations of human parameters are not completely random in short-term observations. According to the experiment results in [27], the human parameters can be continuously smaller or greater than their overall mean values for tens of second, which is long enough to cause unexpected consequences (such as loss of string stability) in vehicle control. An example in daily life is that driver would change the aggressiveness depending on congestion level.

Therefore, a more realistic yet convenient assumption is that the human driver responds to each speed perturbation from the downstream in different ways, but the driver's behavior during one regulation period is relatively stable. This assumption implies that any control design involving human driver should be able to handle a range of human parameters instead of a specific combination, because those human parameters may significantly change from what they used to be. Meanwhile, (1) can still be considered as a locally linear time-invariant system in each period of regulation (so transfer function exists), which will bring great convenience in the string stability analysis.

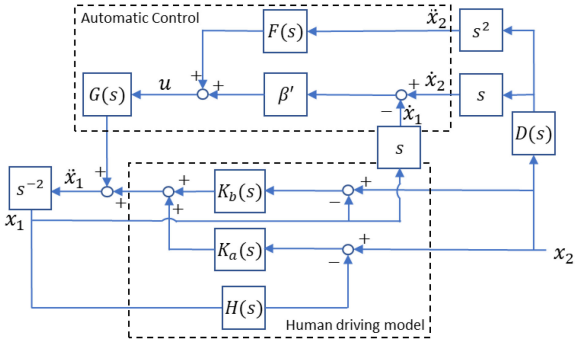

Fig. 2. Control diagram of hCCC.

B. High-Level Control

Since human driving has already included feedback control in terms of spacing and speed, a natural approach is giving an additional acceleration feedforward to the ego vehicle (which is similar to upgrading ACC to CACC). Besides, as human's feedback control has long delay, it will be desirable to have an automatic speed feedback which can more timely capture the speed difference from the preceding vehicle. Therefore, the car-following behavior of hCCC vehicle is decided as:

$$h\left(t\right) = x_2\ \left(t\right) - x_1\left(t\right) - l$$
$$\ddot{x}_1\left(t\right) = \alpha\left(\frac{1}{t_h}h\left(t-\varphi\right) - \dot{x}_1\left(t-\varphi\right)\right) + \beta\dot{h}\left(t-\varphi\right) + g\left(u\left(t\right)\right)$$
$$u\left(t\right) = \beta'\left(x_2\left(t-\theta\right) - x_1\left(t\right)\right) + f\left(\ddot{x}_2\right) \quad (2)$$

Where φ, α, β and t_h are human parameters, u is the acceleration command made by the high-level controller; $g(u(t))$ represents the actual acceleration achieved by the longitudinal vehicle dynamics; β' is the control gain for the automatic speed feedback; $f(\ddot{x}_2)$ denotes a linear feedforward filter that generates commands based on the received acceleration of preceding vehicle; θ is the communication delay.

By taking Laplace transform of (2), a control diagram of hCCC can be depicted in Fig. 2, where:

$$K_a\left(s\right) = \frac{\alpha}{t_h}e^{-\varphi s}, K_b\left(s\right) = \beta s e^{-\varphi s}, H\left(s\right) = 1 + t_h s,$$
$$K_b\left(s\right) = \beta s e^{-\varphi s}, D\left(s\right) = e^{-\theta s}.$$

And $G(s)$ and $F(s)$ are Laplace transforms of $g(u(t))$ and $f(\ddot{x}_2)$; s is the Laplace variable. Accompanied by a proper low-level controller as shown later, the longitudinal vehicle dynamics can be approximated by a first-order system:

$$g\left(u\left(t\right)\right) + \tau\dot{g}\ \left(u\left(t\right)\right) = \ u\left(t - \emptyset\right) \quad (3)$$

In time domain and a transfer function:

$$G\left(s\right) = \frac{1}{1+\tau s}e^{-\emptyset s} \quad (4)$$

In Laplace domain.

Where τ and $\varnothing$ are the response lag and actuator delay of the ego vehicle, respectively.

The feedforward filter $F(s)$ is designed to pre-compensate spacing error introduced by the speed perturbation of the preceding vehicle. We denote spacing error:

$$e_h(t) = h(t) - t_h \dot{x}_1(t) \tag{5}$$

Then the Laplace transform of spacing error can be derived by combining (2) and (5), as shown in (6) at the bottom of this page.

Where $K_b' = \beta' s$; E_h(s) and $X_2(s)$ are the Laplace transforms of spacing error and location of the preceding vehicle, respectively. To make $E_h(s) = 0$ for any $X_2(s)$, the ideal feedforward filter $F(s)$ is:

$$F(s) = \frac{1 - t_h\left(\beta e^{-\varphi s} + \beta' G(s)\right)}{H(s) G(s) D(s)}$$

Considering that the exact values of human parameters t_h, β, φ, and communication delay θ cannot be obtained, an approximated feedforward filter is given by:

$$F(s) = \frac{1 - \bar{t}_h \beta' G(s)}{(1 + \bar{t}_h s) G(s)} \tag{7}$$

Where $\bar{t}_h$ is the mean value of t_h over the past time. It can be estimated using the method proposed in [27]. An important assumption applied to the derivation of (7) is that the human driver tends to deactivate his own speed feedback control when an automatic speed feedback control is present, i.e., $\beta \to 0$ if $\beta' > 0$. This assumption is based on our observations in preliminary experiments of hCCC and to be further verified in Section IV.

For comparison, the car-following behavior of the acceleration-based CCC [22] is given by:

$$\begin{aligned} h(t) &= x_2(t) - x_1(t) - l \\ \ddot{x}_1(t) &= \alpha\left(\frac{1}{t_h} h(t-\varphi) - \dot{x}_1(t-\varphi)\right) + \beta \dot{h}(t-\varphi) + g(u(t)) \\ u(t) &= \gamma \ddot{x}_2(t-\theta) \end{aligned} \tag{8}$$

Where γ is the constant gain for acceleration feedforward in CCC, and $\gamma = 0.5$ is usually chosen to obtain the best performance [22]. Accordingly, the control diagram of this CCC can be given by replacing F with γ, and letting $\beta' = 0$ in Fig. 2.

C. Low-Level Control

The output of high-level controller is the extra desired acceleration of the vehicle. However, the longitudinal motion of vehicle is directly controlled by the throttle and brake. Thus, a low-level controller is needed to convert the desired acceleration to proper throttle and brake action so that the command from high-level controller can be accurately achieved. A well-accepted version of low-level controller [28] for ACC/CACC utilizes the inverse engine torque map and a set of feedforward signals (i.e., vehicle speed, engine speed, transmission ratio) to pre-compensate the nonlinearity of the engine, transmission system, air drag and rolling resistance, leading to a first-order linear relationship between desired acceleration and actual acceleration as described by (3) and (4). However, the case of hCCC is slightly different. The desired acceleration of the controller should be added onto human's action, not actuating the vehicle alone. Therefore, the throttle and brake generated by the existing low-level controller cannot be directly used. Instead, the modification on human's throttle/brake input should be further decided.

The goal of low-level controller is to make the vehicle acceleration as close as possible to the summed demands of human driver and high-level controller:

$$\ddot{x}_1 \to u_h + u \tag{9}$$

Where u_h is the intended acceleration by human driver, and u is the desired extra acceleration by hCCC high-level control. To achieve (9), we need:

$$gl(th_h + \Delta th, br_h + \Delta br) = u_h + u \tag{10}$$

Where $gl(\cdot)$ denotes the low-level vehicle dynamics model that maps throttle/brake input to the vehicle acceleration. th_h/br_h is the throttle/brake input by the human; $\Delta th/\Delta br$ is the modification on throttle/brake to be determined. While $gl(\cdot)$ is a nonlinear function, it can be known as the inverse of low-level controller in [28]. Since th_h and br_h can be sensed through throttle and brake pedal, human's intention u_h can also be computed:

$$u_h = gl(th_h, br_h) \tag{11}$$

Then, the new low-level control law can be derived combining (10) and (11):

$$(\Delta th, \Delta br) = gl^{-1}(gl(th_h, br_h) + u) - (th_h, br_h) \tag{12}$$

Where gl^{-1} is right the low-level controller in [28].

In the following analysis and evaluations, the ego vehicle will be presented by an Audi A8 sedan model from PreScan [29]. This physics-based vehicle model consists of engine, automatic gear box, 2-D chassis and other typical vehicle components. With the low-level controller (12), the first-order vehicle dynamics can be identified from the vehicle's response given step acceleration commands [30]. MATLAB system identification toolbox is adopted to accomplish this identification. The identification result is:

$$G(s) = \frac{1}{1 + 0.12s} e^{-0.2s} \tag{13}$$

$$E_h(s) = \left(1 - \frac{H(s)\left(K_b(s) + K_a + G(S) D(s)\left(s^2 F(s) + K_b'(s)\right)\right)}{s^2}\right) X_2(s) \tag{6}$$

III. String Stability Analysis

A. String Stability Criterion

String stability is one of the most important design goals of longitudinal vehicle control. Although string stability can be defined as either head-to-tail wise or pair wise, this study keeps the consistency with the typical decentralized CACC designs [2], [31], [32] which pursue pair-wise string stability (also referred to as strong string stability), because it automatically fulfills head-to-tail string stability (also referred to as weak string stability) when forming a platoon of such vehicles.

A widely-accepted version of pair-wise string stability is defined in [32], that is, given any disturbance in the longitudinal movement of preceding vehicle, the following vehicle should not amplify this disturbance. While string stability can also be defined in terms of spacing error or control input, they are less practical when human driver is involved. According to [32], the string stability of ego vehicle is fulfilled when the frequency response magnitude of its transfer function is no greater than 1:

$$SS = \|T(j\omega)\|_\infty = \left\| \frac{X_1(j\omega)}{X_2(j\omega)} \right\|_\infty \leq 1 \tag{14}$$

Where $T(*)$ is the transfer function of the vehicle. X_1 and X_2 are the Laplace transforms of locations of the ego vehicle and preceding vehicle, respectively. $\| * \|_\infty$ denotes the maximum magnitude for all frequencies $\omega > 0$, and j is an imaginary unit. Denoting $L(*)$ as the Laplace transform operation, we have $\frac{X_1(s)}{X_2(s)} = \frac{L(x_1(t))}{L(x_2(t))} = \frac{L(\dot{x}_1(t))}{L(\dot{x}_2(t))} = \frac{L(\ddot{x}_1(t))}{L(\ddot{x}_2(t))}$. Thus, condition (14) can be approximately interpreted as that the speed or acceleration peak value of ego vehicle should not exceed that of the preceding vehicle.

B. Plant Stability Requirement

It should be noticed that the string stability described by (14) does not necessarily guarantee the stability of individual vehicle or so called "plant stability", or simply "stability" (i.e., the capability of asymptotically recovering to a steady state after a disturbance) [22]. Plant stability is the very basic requirement for a physical system to survive in real world. Instability causes unbounded self-oscillation and eventually damages the system [33]. For a plant-stable system, the poles of its transfer function (i.e., zeros of the denominator) should have negative real parts [33].

According to (1), the transfer function of human-driven vehicle without any automatic control is:

$$T(s) = \frac{K_a + K_b}{s^2 + K_b + HK_a} \tag{15}$$

For CCC, the transfer function can be derived from (8):

$$T(s) = \frac{K_a + K_b + 0.5s^2GD}{s^2 + K_b + HK_a} \tag{16}$$

For hCCC, the transfer function can be derived from (2) and (7):

$$T(s) = \frac{H(K_a + K_b) + \left(s^2 + GK_b'\right) D}{H(s^2 + K_b + GK_b' + HK_a)} \tag{17}$$

Human driving (15) and CCC (16) have the same denominator, as CCC only gives an open-loop control command (see $u(t)$ in (8)). Their plant stability boundaries have been derived in [22] by making the denominator of $T(j\omega)$ equal zero:

$$\begin{aligned} \alpha &= t_h\omega^2 \cos(\varphi\omega) \\ \beta &= \omega \sin(\varphi\omega) - \alpha \end{aligned} \tag{18}$$

As for hCCC (17), the denominator is different since the command of hCCC includes a closed-loop speed feedback (see $u(t)$ in (8)) which depends on ego vehicle's state. In the same way with [22], the plant-stable boundaries for hCCC can be derived:

$$\begin{aligned} \alpha &= t_h(\omega^2 \cos(\varphi\omega) + \beta'\omega \sin(\varphi\omega)) \\ \beta &= \omega \sin(\varphi\omega) - \beta'\omega \cos(\varphi\omega) - \alpha \end{aligned} \tag{19}$$

Therefore, to make the string stability (14) meaningful, the human parameters in $T(s)$ must be on the stable side of the plant stability boundaries (18) or (19).

C. String-Stable Ranges of Human Parameters

As aforementioned, the human parameters $\alpha,\ \beta,\ \mathrm{t_h},\ \varphi$ are likely to vary over time. For a better robustness, hCCC should be able to work properly when there is a discrepancy between the expected $\alpha,\ \beta,\ \mathrm{t_h},\ \varphi$ and the actual values.

The realistic ranges of human parameters have been investigated in previous studies:

- The preferred time gap t_h of highway drivers is found to be 1∼2s [34].
- The human delay φ was reported to be 0.5∼1.5s in [35], while [36] found the brake delay in normal case to be 0.92∼1.93s, and acceleration delay to be 0.4∼1.5s.
- As for the human control gains α and β, previous literature [22], [37] used the average value of 0.6 and 0.9, which are derived from macroscopic data. However, field test [38] determined the average values of α_1 and β_1 to be 0.2 and 0.4. We assumed average values of α and β to be 0.4 and 0.65, respectively as compromise.

Next, we demonstrate the theoretical performance of human driving alone, CCC and hCCC by showing the ranges of human parameters which fulfill string stability. Such ranges can be computed based on (14)∼(17), in which the vehicle dynamics $G(s)$ follow (13) and an average communication delay of 100ms [26] is assumed. While other vehicle dynamics and communication delays can also be used for this analysis, they show the similar pattern with the presented results.

Generally speaking, broader string-stable ranges of human parameters (within the plant stability boundaries) indicate better chance to make the vehicle stay string-stable under various human behaviors.

By fixing desired time gap and human delay at their average values, i.e., $(t_h,\ \varphi) = (1.5,\ 1)$, Fig. 3(a), (b), (c) show string-stable ranges (blank area) of $\alpha,\ \beta$ for human driving, CCC and hCCC, respectively. Then, fixing human gains at their average values, i.e., $(\alpha,\ \beta) = (0.4,\ 0.65)$, Fig. 3(d), (e) show string-stable ranges of $t_h,\ \varphi$ for human driving and CCC. Lastly,

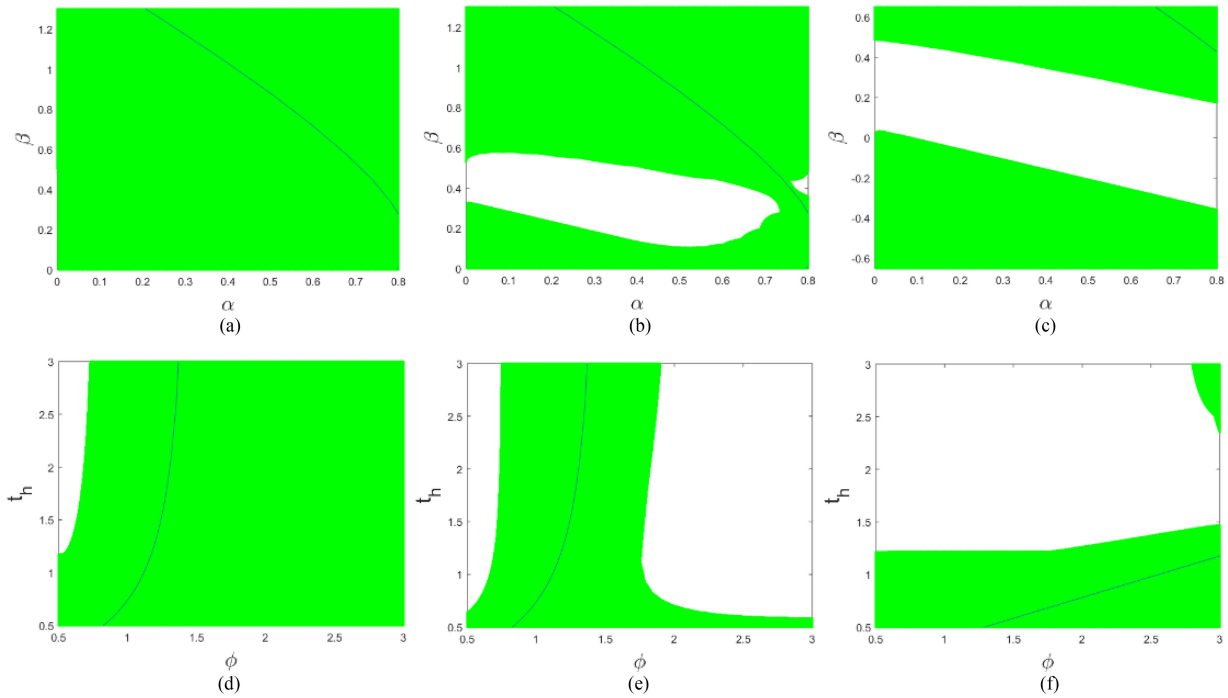

Fig. 3. String-stable ranges (blank areas) of human parameters and plant stability boundaries (solid lines) under different controls. (a) Human driving. (b) CCC. (c) hCCC. (d) Human driving. (e) CCC. (f) hCCC.

Fig. 3(f) shows string-stable ranges of $t_h,\ \varphi$ for hCCC when fixing $(\alpha,\ \beta)\ =\ (0.4,\ 0)$. The plant stability boundaries are plotted in solid lines, of which the left side represents plant-stable areas.

In human driving (Fig. 3(a), (d)), no positive α or β can be found to fulfill string stability when $(t_h,\ \varphi)\ =\ (1.5,\ 1)$. To make the vehicle string-stable with $(\alpha,\ \beta)\ =\ (0.4,\ 0.65)$, human delay should be no longer than 0.7s.

According to Fig. 3(b), (e), CCC offers broader string-stable ranges of $\alpha,\ \beta$ than human driving does. Besides, shorter time gap (e.g., 0.6s) is allowed but only in case of very small human delay (e.g., 0.5s). Although CCC could regain the string stability when human delay (φ) exceeds 2s, it is meaningless as plant stability would have been violated.

For hCCC (Fig. 3(c), (f)), $\beta' =\ 0.65$ and $\bar{t}_h =\ 1.5$ are used in the high-level controller. Obviously, hCCC owns much broader string-stable ranges of human parameters than CCC does. Fig. 3(c) shows that α can be almost any positive value when $\beta\ =\ 0$. In fact, residual β does not need to be exactly 0, because a broad "buffer area" around $(\alpha,\ \beta)\ =\ (0.4,\ 0)$ is provided. Fig. 3(f) further shows that a vast range of time gaps can be used under any human delay $<$ 3s without violating plant stability.

In addition, although hCCC requires the estimated $\bar{t}_h$ in (7), it has significant tolerance on the discrepancy between the estimated $\bar{t}_h$ and the actual t_h. This makes the possibility to further loose the operating condition of hCCC. Since $\bar{t}_h$ is the only human parameter needed in the configuration of hCCC, it is worth exploring whether hCCC can perform similarly well when replacing estimated $\bar{t}_h$ with a pre-tuned constant t_c. If this works, hCCC can be a generic control design instead of being user-specific, and also become more suitable for large-scale implementation due to the cancellation of human parameters estimation which requires minutes to be done [27].

A desirable t_c should give hCCC vehicle a good chance to stay string-stable when co-piloting under various human driving behaviors. To do so, String Stability Ratio (SSR) is defined as the probability that hCCC vehicle can stay string-stable given all different kinds of $(\alpha, \beta, \varphi,\ t_h)$. It can serve as a performance measure of the hCCC's robustness against human parameters variation. By definition, SSR can be computed as an integral of the probability density of all string-stable combinations of $(\alpha, \beta, \varphi,\ t_h)$:

$$SSR\ = \int\int\int\int f\left(\alpha, \beta, \varphi,\ t_h\right) \xi\left(SS\right) d\alpha d\beta d\varphi dt_h \tag{20}$$

Where

$$\xi\left(SS\right) = \begin{cases} 1 & \text{if } SS \leq 1 \\ 0 & \text{if } SS > 1 \end{cases} \tag{21}$$

SS is the string stability determinant that can be calculated through (14) and (17). $f(\alpha, \beta, \varphi,\ t_h)$ is the joint probability density function (PDF) of human parameters. Assuming independent distributions of human parameters [38], we have

$$f\ \left(\alpha, \beta, \varphi,\ t_h\right) =\ f\left(\alpha\right) f\left(\beta\right) f\left(\varphi\right) f\left(t_h\right) \tag{22}$$

Where $f(\alpha), f(\beta), f(\varphi), f(t_h)$ are the PDF of $\alpha, \beta, \varphi,\ t_h$, respectively. To obtain $f(\alpha), f(\beta), f(\varphi), f(t_h)$ and thus complete the configuration of pre-tuned hCCC, the distributions of human parameters under the effect of hCCC need to be collected. Note that the human parameters reported in previous references [22],

[34]–[38] is not directly usable, because the human's behavior with hCCC may be different from that when driving alone.

IV. Evaluation

The purpose of the evaluation is threefold:

- Verify hCCC's performance over human driver and CCC;
- Confirm the validity of the assumption that human drivers would tend to deactivate their own speed feedback control during the onset of hCCC;
- Explore the effectiveness of derivative designs of hCCC.

There are two derivative designs of hCCC considered here: the aforementioned pre-tuned hCCC and semi-hCCC which only adjusts throttle but not brake of the vehicle. This semi- hCCC is to incorporate the fact that there are still many old or low-cost vehicles equipped with only electronic throttle but no electronic brake or ESP/ESC that support programmed brake for driver assistance system. Therefore, semi-hCCC is proposed to lower down the hardware threshold of hCCC for such vehicles.

Three rounds of driving simulator tests are conducted based on the evaluation purposes. In the first round, the participants drive with hCCC, CCC, and no-automation, respectively, through which the performance of hCCC can be quantified. Meanwhile, the distributions of human parameters in the hCCC runs are estimated, in order to validate the assumption on human's feedback, and to complete the configuration of pre-tuned hCCC. In the second round of tests, the pre-tuned hCCC and semi-hCCC are compared with the standard hCCC, to investigate how worse or better hCCC can do without human parameter estimation or automatic brake, respectively. In the last round of tests, the pre-tuned hCCC is implemented to a 4-vehicle platoon, to demonstrate its generality and platoon-wise benefits.

The measures of effectiveness (MOEs) are defined in three aspects:

- Safety: Time Exposed Time-to-collision (TET) [39] is adopted as a surrogate measure for safety performance. TET is calculated by accumulating the time periods when the vehicle is exposed to an unsafe Time-to-Collision (TTC):

$$TET = \int \delta_i(t)\, dt$$

$$\delta_i t = \begin{cases} 1, & \text{if } TTC < TTC^* \\ 0, & \text{otherwise} \end{cases}$$

$$TTC = h(t) / \dot{h}(t) \tag{23}$$

Where TTC^* is a threshold for unsafe *TTC*. According to NHTSA, TTC $<$ 2s is considered a situation dangerous enough to activate Forward Collision Warning (FCW) system [40]. Therefore, $TTC^*$is chosen be to 2s in this study.

- Energy efficiency. Fuel consumption of the vehicle in each run is estimated using VT-micro fuel consumption model [41].
- Traffic disturbance. The root mean square (RMS) of acceleration and standard deviation (STD) of time gap are collected to quantify the speed/spacing disturbances the ego vehicle undergoes;

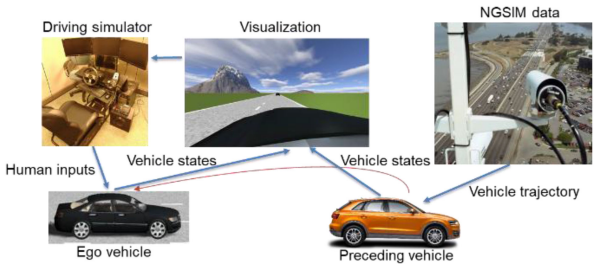

Fig. 4. Overview of the experiment.

In addition to the numerical measures, string stability of the vehicle can be directly judged by comparing the speed/acceleration profile with preceding vehicle's and checking for speed/acceleration overshootings.

A. Experiment Set-Up

As shown in Fig. 4, the experiment combines an off-the-shelf software PreScan, the real traffic data from Next Generation SIMulation (NGSIM) program, and a driving simulator with Logitech hardware.

1) PreScan and Control Systems: PreScan is a simulation platform designed for evaluating Advanced Driver Assistance Systems (ADAS). In this study, it offers simulation environment and physics-based vehicle dynamics model. A straight-highway car-following scenario is developed and visualized in driver's view via PreScan. This driver's view is updated in 20 Hz and projected to the screen (windshield) of the driving simulator so that the participant can perceive the situation and take actions on throttle/brake pedal and steering wheel. These actions are then fed back to PreScan. Using the vehicle dynamics model embedded, PreScan can calculate how the driver's actions, along with hCCC/CCC, change the status of the ego vehicle and reflect the change in the driver's view.

As noted, the control system for ego vehicle is divided into high-level and low-level controllers. There are two high-level controllers (i.e., hCCC and CCC) to be evaluated, while the low-level system remains the same. The V2V communication delay is assumed to be 100ms throughout the evaluation.

2) Predecessor Driving Behavior: To make the evaluation more realistic, the speed profile of preceding vehicle is derived from the real-world vehicle trajectory data of Next Generation Simulation (NGSIM) program [42], which was launched by the Federal Highway Administration (FHWA). NGSIM used high-resolution cameras to record trajectories of the vehicles on real roads. The US Highway 101 (US 101) dataset was one dataset that reflected highway traffic condition. It contains the location and speed profiles of vehicles in all 6 lanes within the 640-meter-long study area during 45 minutes. Due to the limited length of the single vehicle's speed profile in the NGSIM data, we link 4 short speed profiles of different vehicles, by constant deceleration of $1m/s^2$, into a 4-minute speed profile as shown in Fig. 5. It should be emphasized that this speed profile is not directly given to the preceding vehicle in the evaluation; instead, it is "tracked" through a PID controller and vehicle dynamics

TABLE I
SUMMARY OF EVALUATION RESULTS

# of Participant		1	2	3	4	5	6	7	8	Mean
hCCC	RMS Acceleration/m/s^2	0.7	0.67	0.73	0.78	0.648	0.57	0.65	0.645	0.67
	Time gap (mean±STD)/s	1.7±0.55	2.03±0.72	1.87±0.56	0.97±0.34	1.55±0.55	1.3±0.55	1.95±0.97	1.74±0.5	1.64±0.59
	TET/s	0	0	0	1.8	0	3.9	0	0	0.7125
	Fuel consumption/L	0.157	0.151	0.161	0.165	0.147	0.14	0.149	0.153	0.15
	RMS throttle/brake	10%/4%	10%/5%	11%/6%	13%/5%	9%/2%	9%/2%	13%/2%	11%/2%	11%/4%
CCC	RMS Acceleration/m/s^2	1.02	0.8	1.24	0.91	1.31	0.83	1.04	1.25	1.05
	Time gap (mean±STD)/s	1.48±1.15	2.24±1.27	1.61±1.08	1.14±0.47	1.39±0.86	1.78±0.81	2.19±1.02	1.56±0.72	1.67±0.93
	TET/s	2.2	6.6	5.3	6.2	8.7	4.6	2.8	5.9	5.3
	Fuel consumption/L	0.171	0.147	0.187	0.16	0.174	0.155	0.163	0.207	0.17
	RMS throttle/brake	15%/13%	13%/9%	16%/16%	15%/11%	16%/16%	14%/9%	16%/14%	17%/16%	15%/13%
Human driving	RMS Acceleration/m/s^2	0.98	0.86	1.36	0.99	1.08	0.99	1.21	1.07	1.07
	Time gap (mean± STD)/s	1.86±1.04	2.74±1.31	2.31±0.85	0.92±0.45	1.93±0.69	1.69±0.73	1.59±1.12	1.39±0.65	1.80±0.86
	TET/s	2.1	3.9	2.6	4.5	1.1	0.6	8.3	7.3	3.8
	Fuel consumption/L	0.154	0.154	0.219	0.163	0.174	0.189	0.197	0.19	0.18
	RMS throttle/brake	14%/12%	13%/10%	16%/17%	17%/11%	15%/13%	17%/11%	17%/16%	16%/12%	16%/13%

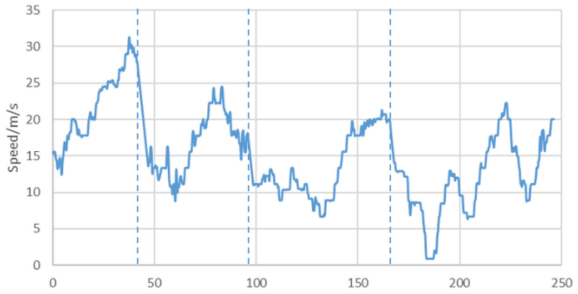

Fig. 5. Desired speed profile of the preceding vehicle.

model. This setting is designed to eliminate the inconsistent speeds and unrealistic jerks (i.e., derivative of acceleration) that frequently occur in the original NGSIM data [43]. The PID controller and the vehicle dynamics model together play as a filter that smooths the trajectory and makes sure the movements are mechanically realistic. To fairly compare the performances of different controls, the trajectory of the preceding vehicle is set to be identical in all the runs.

3) Human Drivers: There are 8 participants in the first round of tests, and 4 in the second round of tests. In the first round, each participant is required to drive the ego vehicle and track the preceding vehicle for 4 runs (each run lasts for 4 minutes): warm-up run, hCCC, CCC, and human driving. The purpose of warm-up run is to familiarize the driver with driving simulator, and estimate the human parameters using the method from [27], after which hCCC can be configured. The warm-up run is always placed the first, while the other 3 runs are randomly sequenced to disperse the driver's learning and fatigue effects. In the second round, there are 4 runs besides warm-up for each participant: human driving, hCCC, pre-tuned hCCC, and semi-hCCC, in a randomized sequence.

B. Results

1) First Round of Tests: The results of the first round of tests are listed in Table I. hCCC reduced 36.8% acceleration, 31.2% time-gap fluctuation, 81.2% exposure time to unsafe driving situations (TET), and 15.8% fuel consumption from those of human driving, respectively. Paired t-test indicates all these benefits are statistically significant. This means hCCC has great potential to mitigate traffic disturbances, avoid unsafe driving condition and save energy. It is noted that these benefits were achieved by hCCC at an even shorter gap than human driving did. It is also observed that under hCCC, human drivers took 31.2% and 64.3% less control effort on throttle and brake levels than in human driving alone, indicating a decrease in labor intensity of the drivers.

When compared with CCC, hCCC reduced 35.8% acceleration, 36.6% time-gap fluctuation, 86.5% exposure time to unsafe driving situations (TET), and 10.3% fuel consumption, showing consistently large improvements.

In contrast, paired t-test indicates that all the resulted MOEs of CCC show no statistically significant difference from those of human driving alone. Thus, there was no performance improvement over human driving achieved by CCC.

Fig. 6 shows the speed and acceleration profiles of the participant 1. Fig. 6(a), (d) are for human driving; (b), (e) are for CCC; and (c), (f) are for hCCC. It is noticed that many speed overshootings occurring in human driving and CCC runs were avoided in hCCC, and the acceleration of hCCC vehicle was mostly smaller than that of the preceding vehicle, indicating an improved string stability. It is noted that string stability is not the only contributing factor to the good performance of hCCC. The results are also largely determined by "how poorly" the hCCC/CCC/human driving performed in string-unstable conditions. When comparing Fig. 6(c) with (a) and (b), it is clear that hCCC not only had the better chance to avoid overshootings, but also greatly suppressed the magnitude of the overshooting when it happens. This finding highlights the importance of experiments with real drivers instead of only looking at theoretical analysis.

2) Driving Behavior With hCCC: Another purpose of the first round of tests was to obtain human parameters under the effect of hCCC so that the assumption can be tested that human's speed feedback can be checked and pre-tuned.

The human parameters in all the runs are estimated using the method in [27] and their mean values (i.e., $\bar{\alpha}$, $\bar{\beta}$, $\bar{\varphi}$ and

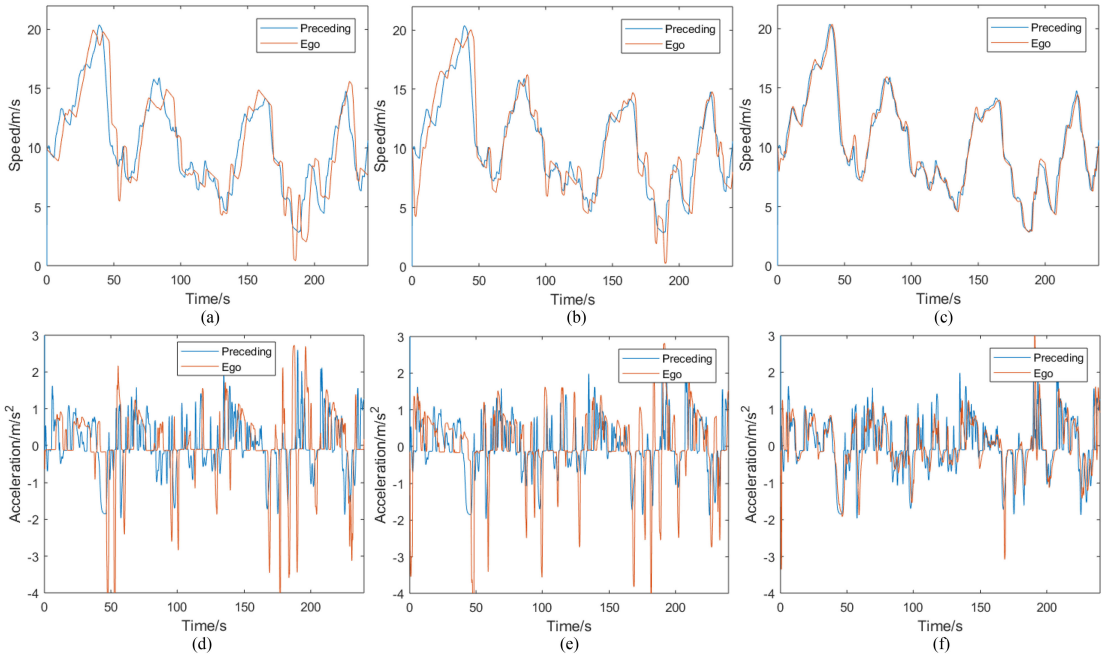

Fig. 6. Speed and acceleration profiles of the participant 1. (a) Human driving. (b) CCC. (c) hCCC. (d) Human driving. (e) CCC. (f) hCCC.

TABLE II
SUMMARY OF ESTIMATED HUMAN PARAMETERS IN ALL RUNS

# of participant		1	2	3	4	5	6	7	8	Mean
hCCC	$\bar{\alpha}$	0.05	0.03	0.06	0.02	0.05	0.03	0.03	0.04	0.04
	$\bar{\beta}$	0.25	0.08	0.14	0.25	0.08	0.06	0.02	0.05	0.12
	$\bar{\varphi}$	1.8	1.66	1.69	1.08	1.38	1.31	1.92	1.63	1.56
	$\bar{t}_h$	1.08	1.46	1.29	0.51	1.16	0.65	1.11	1.08	1.04
CCC	$\bar{\alpha}$	0.08	0.06	0.09	0.04	0.11	0.1	0.09	0.14	0.09
	$\bar{\beta}$	0.45	0.17	0.47	0.44	0.42	0.25	0.3	0.27	0.35
	$\bar{\varphi}$	1.31	1.44	1.19	1.11	1.32	1.19	1.56	1.29	1.30
	$\bar{t}_h$	0.76	1.52	0.85	0.69	0.69	1.2	1.48	0.93	1.02
Human driving	$\bar{\alpha}$	0.1	0.06	0.2	0.06	0.1	0.1	0.09	0.13	0.11
	$\bar{\beta}$	0.3	0.2	0.34	0.62	0.31	0.38	0.37	0.3	0.35
	$\bar{\varphi}$	1.24	1.68	1.37	1.04	1.29	1.25	1.18	1.25	1.29
	$\bar{t}_h$	1.16	2.09	1.77	0.48	1.21	1.1	0.95	0.9	1.21

$\bar{t}_h$) are listed in Table II. In average, $\bar{\beta}$ under hCCC is only 33% of what it used to be in the human driving. This proves our assumption reasonable and explains the favorable performance of hCCC, which needs the residual β to be small. In addition, each driver showed different human parameters with or without CCC. It does challenge the fundamental assumption CCC adopted that human behaves the same even with the help of ADAS.

As noted, the pre-tuning of hCCC requires the probability density function (PDF) of human parameters under the effect of hCCC. Fig. 7 shows the distributions of estimated α, β, t_h, φ in the human driving runs (in Fig. 7(a)∼(d)), and those in the hCCC runs (in Fig. 7(e)∼(h)), respectively. Generally speaking, the human behavior under hCCC was quite different from driving alone. It can be seen that hCCC shifts the distributions of human gains α, β to the left, and α, β have significantly high frequencies to be zero. In addition, the human delay under hCCC tends to be either extremely short or extremely long, while in human driving runs the human delay is concentrated between 0.5s and 1.5s.

While different distributions of human parameters and t_c may be obtained when more data is available, the estimated α, β, t_h, φ in the 8 hCCC runs are fitted into PDFs of kernel distributions. With these PDFs, the optimal $t_c = 1s$ can be found to achieve the maximum SSR $= 28\%$, which is the probability to secure string stability.

3) Second Round of Tests: The evaluation of semi-hCCC and pre-tuned hCCC were conducted with another four participants, and the results are summarized in Table III. The results of human driving and standard hCCC (with human parameters estimation) were also reported to facilitate easier comparison.

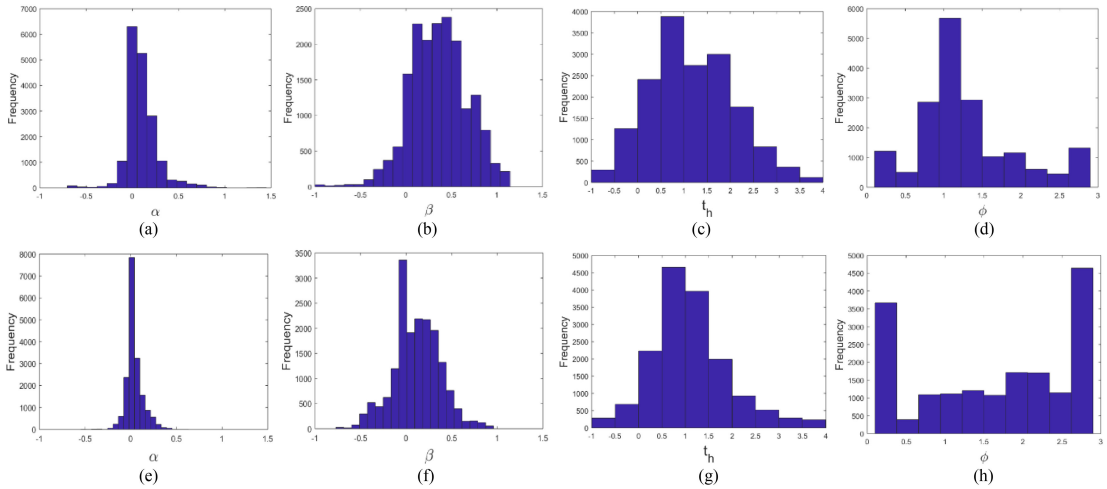

Fig. 7. Distribution of estimated human parameters in human driving and hCCC.

TABLE III
EVALUATION RESULTS OF PRE-TUNED hCCC AND SEMI-hCCC

# of participant		1	2	3	4	Mean
Standard hCCC	RMS acceleration/m/m^2	0.87	0.63	0.78	0.96	0.81
	Time gap STD/s	0.65	0.42	0.41	0.39	0.47
	TET/s	0	0	0	7.7	1.93
	Fuel consumption/L	0.155	0.119	0.129	0.146	0.14
Pre-tuned hCCC	RMS acceleration/m/s^2	0.93	0.65	0.82	0.86	0.82
	Time gap STD/s	0.5	0.48	0.44	0.34	0.44
	TET/s	0	0	0.6	1.4	0.50
	Fuel consumption/L	0.157	0.121	0.127	0.147	0.14
Semi-hCCC	RMS acceleration/m/s^2	1.11	0.74	0.97	1.08	0.98
	Time gap STD/s	0.67	0.48	0.39	0.26	0.45
	TET/s	0	1.7	0.2	4.7	1.65
	Fuel consumption/L	0.163	0.124	0.125	0.171	0.15
Human driving	RMS acceleration/m/s^2	1.76	0.87	2.04	0.98	1.41
	Time gap STD/s	0.95	0.51	0.8	0.31	0.64
	TET/s	0	1.2	9	4.9	3.78
	Fuel consumption/L	0.273	0.145	0.28	0.154	0.21

It can be seen that there were no significant differences between the performances of hCCC and pre-tuned hCCC in all aspects, which means the time-consuming human parameters estimation can be omitted in the implementation of hCCC. This finding makes hCCC easier to be implemented.

Meantime, semi-hCCC had similar performances in time gap STD, TET, and fuel consumption with hCCC. Although its RMS acceleration is 20% higher than standard hCCC, it is still 30% lower than the human driving baseline. Therefore, semi-hCCC is a good alternative for vehicles without electronically controllable brake.

4) Third Round of Tests: Lastly, the pre-tuned hCCC was tested in a platoon wise. In these tests, the leading vehicle still followed NGSIM data, and the following three vehicles were driven by different volunteers. Because the driving simulator can only accommodate one person at a time, the trajectories of the three following vehicles were generated one by one by the volunteers. For example, the NGSIM data played as the preceding vehicle when the 1st volunteer drove, and then vehicle trajectory generated by the 1st volunteer played as the preceding vehicle when the 2nd volunteer drove, and so forth. It is noted that the same pre-tuned hCCC were applied to the different volunteers without adjustment.

The speed profiles of the platooned vehicles under hCCC and those under human driving as baseline are shown in Fig. 8. It can be seen that the traffic disturbances were amplified by the human driving but mitigated by the hCCC. When looking at the last vehicle in the platoons, the hCCC reduced 50% fuel consumption and 100% TET from those of human driving. These improvements (especially in fuel saving) are much greater than that in the individual-vehicle tests.

These platoon-wise benefits are as expected and can be interpreted as cumulative effects of individual vehicles in the platoon. The hCCC vehicles with pair-wise string stability perform better than their preceding vehicles and naturally makes the whole

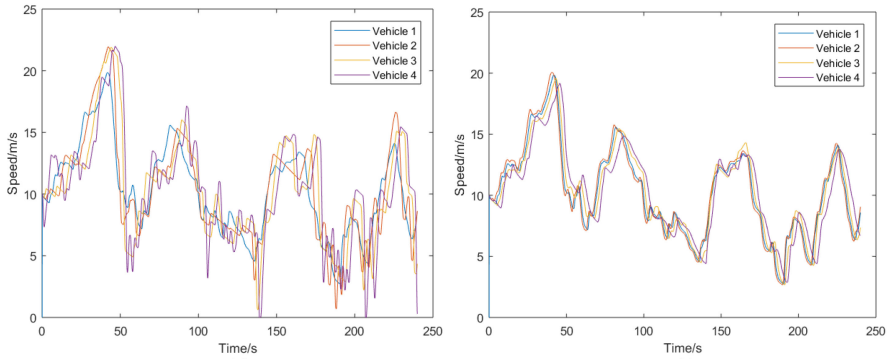

Fig. 8. Speed profiles of 4 platooned vehicle under human driving and hCCC. (a) Human driving. (b) hCCC.

string stable, while human-driving-alone vehicles make the situation worse and worse.

V. Conclusion and Future Work

In this research, an advanced driving assistance system, named human-in-the-loop CACC (hCCC), is proposed. This system can realize machine-human co-piloting and enables a connected-but-not-automated vehicle to perform platooning and improve string stability. In this design, human driver is still engaged in the control of the vehicle, while hCCC serves as an assistant and imposes control adjustments to help driver stabilize the vehicle. The hCCC controller is designed to be bi-level in order to realize control linearization. It also inherits features from conventional CACC, such as feedback-feedforward control structure and zero-spacing-error rule. The proposed hCCC was evaluated against human driver and CCC. The results demonstrated that with the broadest string-stable ranges of human parameters, hCCC had better robustness against the uncertainty of human behaviors. The proposed hCCC was also evaluated with driving simulator experiments to quantify the benefit when used by real human drivers. The results shown that hCCC reduced 36.8% acceleration, 81.2% exposure to unsafe driving situations, 15.8% fuel consumption and 31.2% time-gap fluctuation from those of human driving, respectively, while CCC showed no significant improvements. Detailed investigation of the evaluation reveals that:

- Humans drive differently under the influence of ADAS.
- The proposed hCCC does not require user-specific parameter fitting. This is because hCCC has a wide string-stable range to tolerate the difference between drivers.
- Even a connected vehicle without automated brake ability can achieve most of hCCC's benefits.

Future research could look into the network-wise impacts of hCCC on mixed traffic, where multiple driving modes (e.g., human driving, ACC, CACC, hCCC) and their interactions need to be considered. Additionally, more sophisticated control methods, such as structured singular value analysis [23] and H_∞ method [44], [45] could be applied for the better robustness against the uncertainty in human behaviors and modelling errors. Field tests with real vehicles is also necessary to confirm the findings from this study.

References

[1] K. Bengler, K. Dietmayer, B. Farber, M. Maurer, C. Stiller, and H. Winner, "Three decades of driver assistance systems: Review and future perspectives," *IEEE Intell. Transp. Syst. Mag.*, vol. 6, no. 4, pp. 6–22, 2014, doi: 10.1109/MITS.2014.2336271.

[2] G. J. L. Naus, R. P. A. Vugts, J. Ploeg, M. J. G. Van De Molengraft, and M. Steinbuch, "String-stable CACC design and experimental validation: A frequency-domain approach," *IEEE Trans. Veh. Technol.*, vol. 59, no. 9, pp. 4268–4279, Nov. 2010, doi: 10.1109/TVT.2010.2076320.

[3] L. E. Peppard, "String stability of relative-motion PID vehicle control systems," *IEEE Trans. Autom. Control*, vol. 19, no. 5, pp. 579–581, Oct. 1974, doi: 10.1109/TAC.1974.1100652.

[4] S. Shladover, D. Su, and X.-Y. Lu, "Impacts of cooperative adaptive cruise control on freeway traffic flow," *Transp. Res. Rec. J. Transp. Res. Board*, vol. 2324, pp. 63–70, 2012, doi: 10.3141/2324-08.

[5] S. Shladover *et al.*, "Cooperative adaptive cruise control (CACC) for partially automated truck platooning: Final report," UC Berkeley: California Partners for Advanced Transportation Technology, Aug. 2018. [Online]. Available: https://escholarship.org/uc/item/260060w4

[6] A. Talebpour and H. S. Mahmassani, "Influence of connected and autonomous vehicles on traffic flow stability and throughput," *Transp. Res. Part C Emerg. Technol.*, vol. 71, pp. 143–163, 2016, doi: 10.1016/j.trc.2016.07.007.

[7] D. Jia, D. Ngoduy, and H. L. Vu, "A multiclass microscopic model for heterogeneous platoon with vehicle-to-vehicle communication," *Transportmetrica B Transp. Dyn.*, vol. 7, pp. 311–335, 2019, doi: 10.1080/21680566.2018.1434021.

[8] B. M. Masini, A. Bazzi, and A. Zanella, "A survey on the roadmap to mandate on board connectivity and enable V2V-based vehicular sensor networks," *Sensors (Switzerland)*, vol. 18, no. 7, 2018, Art. no. 2207, doi: 10.3390/s18072207.

[9] P. Bansal and K. M. Kockelman, "Forecasting Americans' long-term adoption of connected and autonomous vehicle technologies," *Transp. Res. Part A, Policy Pract.*, vol. 95, pp. 49–63, 2017, doi: 10.1016/j.tra.2016.10.013.

[10] J. Li, "Roadmap 2.0 for energy-saving and alternative energy vehicle," MIIT and China-SAE. Shanghai, China, 2020. [Online]. Available: http://zhishi.sae-china.org/ppt.html?id=2100

[11] H. Liu, X. (David) Kan, S. E. Shladover, X. Y. Lu, and R. E. Ferlis, "Modeling impacts of cooperative adaptive cruise control on mixed traffic flow in multi-lane freeway facilities," *Transp. Res. Part C Emerg. Technol.*, vol. 95, pp. 261–279, 2018, doi: 10.1016/j.trc.2018.07.027.

[12] J. I. Ge, S. S. Avedisov, C. R. He, W. B. Qin, and M. Sadeghpour, "Experimental validation of connected automated vehicle design among human-driven vehicles," *Transp. Res. Part C Emerg. Technol.*, vol. 91, pp. 335–352, 2018, doi: 10.1016/j.trc.2018.04.005.

[13] I. J. Reagan, D. G. Kidd, and J. B. Cicchino, "Driver acceptance of adaptive cruise control and active lane keeping in five production vehicles," in *Proc. Hum. Factors Ergonom. Soc. Annu. Meeting,* 2017, pp. 1949–1953, doi: 10.1177/1541931213601966.

[14] S. E. Shladover, C. Nowakowski, X.-Y. Lu, and R. Ferlis, "Cooperative adaptive cruise control: Definitions and operating concepts," *Transp. Res. Rec.*, vol. 2489, no. 1, pp. 145–152, 2015.

[15] H. Rakha and R. K. Kamalanathsharma, "Eco-driving at signalized intersections using V2I communication," in *Proc. 14th Int. IEEE Conf. Intell. Transp. Syst.*, 2011, pp. 341–346, doi: 10.1109/ITSC.2011.6083084.

[16] B. L. Smith and H. Park, "Investigating benefits of intellidrive in freeway operations: Lane changing advisory case study," *J. Transp. Eng.*, vol. 138, no. 9, pp. 1113–1122, 2012.
[17] H. S. Tan and J. Huang, "DGPS-based vehicle-to-vehicle cooperative collision warning: Engineering feasibility viewpoints," *IEEE Trans. Intell. Transp. Syst.*, vol. 7, no. 4, pp. 415–428, Dec. 2006, doi: 10.1109/TITS.2006.883938.
[18] J. Deur, D. Pavković, N. Perić, M. Jansz, and D. Hrovat, "An electronic throttle control strategy including compensation of friction and limp-home effects," *IEEE Trans. Ind. Appl.*, vol. 40, no. 3, pp. 821–834, May/Jun. 2004, doi: 10.1109/TIA.2004.827441.
[19] Bosch, "ESP module," Accessed on: May 23, 2022. [Online]. Available: https://www.bosch-mobility-solutions.com/en/solutions/driving-safety/esp-module/
[20] W.-D. Jonner, H. Winner, L. Dreilich, and E. Schunck, "Electrohydraulic brake system - The First approach to brake-by-wire technology," vol. 105, pp. 1368–1375, 1996, doi: 10.4271/960991.
[21] W. Xiang, P. C. Richardson, C. Zhao, and S. Mohammad, "Automobile brake-by-wire control system design and analysis," *IEEE Trans. Veh. Technol.*, vol. 57, no. 1, pp. 138–145, Jan. 2008, doi: 10.1109/TVT.2007.901895.
[22] J. I. Ge and G. Orosz, "Dynamics of connected vehicle systems with delayed acceleration feedback," *Transp. Res. Part C Emerg. Technol.*, vol. 46, pp. 46–64, 2014, doi: 10.1016/j.trc.2014.04.014.
[23] D. Hajdu, J. I. Ge, T. Insperger, and G. Orosz, "Robust design of connected cruise control among human-driven vehicles," *IEEE Trans. Intell. Transp. Syst.*, vol. 21, no. 2, pp. 749–761, Feb. 2020, doi: 10.1109/TITS.2019.2897149.
[24] J. I. Ge and G. Orosz, "Optimal control of connected vehicle systems with communication delay and driver reaction time," *IEEE Trans. Intell. Transp. Syst.*, vol. 18, no. 8, pp. 2056–2070, Aug. 2017, doi: 10.1109/TITS.2016.2633164.
[25] L. Zhang and G. Orosz, "Motif-based design for connected vehicle systems in presence of heterogeneous connectivity structures and time delays," *IEEE Trans. Intell. Transp. Syst.*, vol. 17, no. 6, pp. 1638–1651, Jun. 2016, doi: 10.1109/TITS.2015.2509782.
[26] A. M. H. Al-Jhayyish and K. W. Schmidt, "Feedforward strategies for cooperative adaptive cruise control in heterogeneous vehicle strings," *IEEE Trans. Intell. Transp. Syst.*, vol. 19, no. 1, pp. 113–122, Jan. 2018, doi: 10.1109/TITS.2017.2773659.
[27] J. I. Ge and G. Orosz, "Connected cruise control among human-driven vehicles: Experiment-based parameter estimation and optimal control design," *Transp. Res. Part C Emerg. Technol.*, vol. 95, pp. 445–459, 2018, doi: 10.1016/j.trc.2018.07.021.
[28] R. Rajamani, *Vehicle Dynamics and Control*. Berlin, Germany: Springer, 2006.
[29] M. Tideman, "Scenario-Based simulation environment for assistance systems," *ATZautotechnology*, vol. 10, no. 1, pp. 28–32, Jan. 2010, doi: 10.1007/BF03247153.
[30] R. Kianfar *et al.*, "Design and experimental validation of a cooperative driving system in the grand cooperative driving challenge," *IEEE Trans. Intell. Transp. Syst.*, vol. 13, no. 3, pp. 994–1007, Sep. 2012, doi: 10.1109/TITS.2012.2186513.
[31] V. Milanés, S. E. Shladover, J. Spring, C. Nowakowski, H. Kawazoe, and M. Nakamura, "Cooperative adaptive cruise control in real traffic situations," *IEEE Trans. Intell. Transp. Syst.*, vol. 15, no. 1, pp. 296–305, Feb. 2014, doi: 10.1109/TITS.2013.2278494.
[32] E. van Nunen, M. R. J. A. E. Kwakkernaat, J. Ploeg, and B. D. Netten, "Cooperative competition for future mobility," *IEEE Trans. Intell. Transp. Syst.*, vol. 13, no. 3, pp. 1018–1025, Sep. 2012, doi: 10.1109/TITS.2012.2200475.
[33] J. C. Doyle, B. A. Francis, and A. R. Tannenbaum, *Feedback Control Theory*. North Chelmsford, MA, USA: Courier Corporation, 2013, pp. 34–37.
[34] T. J. Ayres, L. Li, D. Schleuning, and D. Young, "Preferred time-headway of highway drivers," in *Proc. ITSC IEEE Intell. Transp. Syst. (Cat. No.01TH8585)*, 2001, pp. 826–829, doi: 10.1109/ITSC.2001.948767.
[35] G. Orosz, R. E. Wilson, and G. Stepan, "Traffic jams: Dynamics and control," *Philos. Trans. Roy. Soc. A, Math. Phys. Eng. Sci.*, vol. 368, no. 1928, pp. 4455–4479, 2010, doi: 10.1098/rsta.2010.0205.
[36] A. Mehmood and S. M. Easa, "Modeling reaction time in car-following behaviour based on human factors," *Int. J. Civil, Environ. Struct. Constr. Archit. Eng.*, vol. 3, no. 9, pp. 325–333, 2009.
[37] J. I. Ge, G. Orosz, D. Hajdu, T. Insperger, and J. Moehlis, "To delay or not to delay—Stability of connected cruise control," in *Time Delay Systems*. Cham, Switzerland: Springer, 2017, pp. 263–282.
[38] J. I. Ge and G. Orosz, "Data-driven parameter estimation for optimal connected cruise control," in *Proc. IEEE 56th Annu. Conf. Decis. Control*, 2017, pp. 3739–3744, doi: 10.1109/CDC.2017.8264208.
[39] M. M. Minderhoud and P. H. L. Bovy, "Extended time-to-collision measures for road traffic safety assessment," *Accident Anal. Prevention*, vol. 33, no. 1, pp. 89–97, 2001, doi: 10.1016/S0001-4575(00)00019-1.
[40] "Forward collision warning system confirmation test," NHTSA, Washington, DC, USA, 2013.
[41] H. A. Rakha, K. Ahn, K. Moran, B. Saerens, and E. Van Den Bulck, "Virginia tech comprehensive power-based fuel consumption model : Model development and testing," *Transp. Res. Part D Transp. Environ.*, vol. 16, no. 7, pp. 492–503, 2011, doi: 10.1016/j.trd.2011.05.008.
[42] V. Alexiadis, J. Colyar, J. Halkias, R. Hranac, and G. McHale, "The next generation simulation program," *ITE J. Inst. Transp. Eng.*, vol. 74, no. 8, pp. 22–26, 2004.
[43] V. Punzo, M. T. Borzacchiello, and B. Ciuffo, "On the assessment of vehicle trajectory data accuracy and application to the next generation SIMulation (NGSIM) program data," *Transp. Res. Part C Emerg. Technol.*, vol. 19, no. 6, pp. 1243–1262, 2011, doi: 10.1016/j.trc.2010.12.007.
[44] S. E. Li, F. Gao, K. Li, L. Wang, K. You, and D. Cao, "Robust longitudinal control of multi-vehicle Systems—a distributed H-Infinity method," *IEEE Trans. Intell. Transp. Syst.*, vol. 19, no. 9, pp. 2779–2788, Sep. 2018, doi: 10.1109/TITS.2017.2760910.
[45] Y. Zheng, S. E. Li, K. Li, and W. Ren, "Platooning of connected vehicles with undirected topologies: Robustness analysis and distributed H-infinity controller synthesis," *IEEE Trans. Intell. Transp. Syst.*, vol. 19, no. 5, pp. 1353–1364, May 2018, doi: 10.1109/TITS.2017.2726038.

Zheng Chen received the B.S. and M.S. degrees in mechanical engineering from Hunan University, Changsha, China, and the Ph.D. degree in civil engineering from the University of Virginia, Charlottesville, VA, USA. He is currently a Research Engineer with PCI Technology Group Co., Ltd., Guangzhou, China. His research interests include dynamics and control of connected vehicle systems.

Byungkyu Brian Park (Senior Member, IEEE) received the B.S. and M.S. degrees in urban engineering from Hanyang University, Seoul, South Korea, and the Ph.D. degree in civil engineering from Texas A&M University, College Station, TX, USA. He is currently a Professor with the Department of Engineering Systems and Environment and a Member of the link Lab, University of Virginia, Charlottesville, VA, USA.

Jia Hu (Member, IEEE) is currently a ZhongTe Distinguished Chair of cooperative automation with the College of Transportation Engineering, Tongji University, Shanghai, China. Before joining Tongji, he was a Research Associate with Federal Highway Administration, USA (FHWA). He is an Associate Editor for IEEE TRANSACTION ON INTELLIGENT VEHICLE, *American Society of Civil Engineers Journal of Transportation Engineering*, IEEE OPEN JOURNAL IN INTELLIGENT TRANSPORTATION SYSTEMS, an Assistant Editor for the *Journal of Intelligent Transportation Systems*, an Advisory Editorial Board Member for the *Transportation Research Part C*, has been an Associate Editor for IEEE Intelligent Vehicles Symposium since 2018, and an Associate Editor for IEEE Intelligent Transportation Systems Conference since 2019. Furthermore, he is a Member of the TRB (a division of the National Academies) Vehicle Highway Automation Committee, Freeway Operation Committee and Simulation subcommittee of Traffic Signal Systems Committee, and a Member of the CAV Impact Committee and Artificial Intelligence Committee of ASCE Transportation and Development Institute.